7-2015

Impaired synaptic development in a maternal immune activation mouse model of neurodevelopmental disorders

Pierluca Coiro
University of Nebraska Medical Center, Omaha, luca.coiro@unmc.edu

Ragunathan Padmashri
University of Nebraska Medical Center, Omaha, p.ragunathan@unmc.edu

Anand Suresh
University of Nebraska Medical Center, Omaha

Elizabeth Spartz
University of Nebraska Medical Center, Omaha

Gurudutt Pendyala
University of Nebraska Medical Center, Omaha, gpendyala@unmc.edu

See next page for additional authors

Published in *Brain, Behavior, and Immunity* 50 (2015), pp. 249–258; doi: 10.1016/j.bbi.2015.07.022

Submitted May 13, 2015; revised July 24, 2015; accepted July 24, 2015; published online July 26, 2015.

Impaired synaptic development in a maternal immune activation mouse model of neurodevelopmental disorders

Pierluca Coiro,[1] Ragunathan Padmashri,[1] Anand Suresh,[1] Elizabeth Spartz,[1] Gurudutt Pendyala,[1] Shinnyi Chou,[2] Yoosun Jung,[1] Brittney Meays,[1] Shreya Roy,[1] Nagsen Gautam,[3] Yazen Alnouti,[3] Ming Li,[2] and Anna Dunaevsky[1]

1 Department of Developmental Neuroscience, Munroe-Meyer Institute, University of Nebraska Medical Center, Omaha, NE 68198
2 Department of Psychology, University of Nebraska–Lincoln, Lincoln, NE 68588
3 Department of Pharmaceutical Sciences, College of Pharmacy, University of Nebraska Medical Center, Omaha, NE 68198

Corresponding author — A. Dunaevsky, Developmental Neuroscience, Munroe-Meyer Institute, University of Nebraska Medical Center, 985960 Nebraska Medical Center, Omaha, NE 68198-5960, USA; *email* adunaevsky@unmc.edu

Abstract
Both genetic and environmental factors are thought to contribute to neurodevelopmental and neuropsychiatric disorders with maternal immune activation (MIA) being a risk factor for both autism spectrum disorders and schizophrenia. Although MIA mouse offspring exhibit behavioral impairments, the synaptic alterations *in vivo* that mediate these behaviors are not known. Here we employed *in vivo* multiphoton imaging to determine that in the cortex of young MIA offspring there is a reduction in number and turnover rates of dendritic spines, sites of majority of excitatory synaptic inputs. Significantly, spine impairments persisted into adulthood and correlated with increased repetitive behavior, an ASD relevant behavioral phenotype. Structural analysis of synaptic inputs revealed a reorganization of presynaptic inputs with a larger proportion of spines being contacted by both excitatory and inhibitory presynaptic terminals. These structural impairments were accompanied by altered excitatory and inhibitory synaptic transmission. Finally, we report that a postnatal treatment of MIA offspring with the anti-inflammatory drug ibudilast, prevented both synaptic and behavioral impairments. Our results suggest that a possible altered inflammatory state associated with maternal immune activation results in impaired synaptic development that persists into adulthood but which can be prevented with early anti-inflammatory treatment.

Keywords: Autism, Dendritic spines, Excitation, Inhibition, Inflammation, Anti-inflammatory

1. Introduction

Neurodevelopmental disorders, such as autism spectrum disorder (ASD) and schizophrenia (SZ) are likely caused by a combination of genetic alterations and environmental insult during early development. Although the genetic contribution to these disorders is indisputable, increasing evidence points to the role of fetal environment (Patterson, 2011; Voineagu et al., 2011; Hagberg et al., 2012; Knuesel et al., 2014). For example, twin studies indicate that concordance for dizygotic twins is much greater than that for siblings (Hallmayer et al., 2011). Further, epidemiological studies show that infections during pregnancy increase the risk of ASD and SZ in the offspring (Atladottir et al., 2010; Brown, 2012). Evidence of immune dysregulation is found in individuals with both disorders; inflammation is present in postmortem brains, and cytokine levels are altered in the blood, brain, and cerebrospinal fluid in ASD and SZ (Vargas et al., 2005; Chez et al., 2007; Patterson, 2009; Morgan et al., 2010; Watanabe et al., 2010; Ashwood et al., 2011; Wei et al., 2011). The maternal immune response with altered levels of cytokines in both the mother and the offspring is thought to be instigating the brain changes and behavioral impairments in these disorders (Girgis et al., 2014).

Animal studies support the link between maternal immune activation (MIA) and behavioral abnormalities. Studies on prenatal exposure of rodents and primates to maternal infection or inflammation have shown that challenged offspring demonstrate altered behavioral phenotypes relevant to ASD and SZ (Borrell et al., 2002; Fatemi et al., 2002; Shi et al., 2003; McAlonan et al., 2010; Ehninger et al., 2012; Malkova et al., 2012; Bauman et al., 2014). While some studies failed to detect signs of inflammation in offspring born to immune-challenged mothers (Willi et al., 2013; Missault et al., 2014)

and even showed reduction in inflammatory cytokines in the periphery (Pacheco-Lopez et al., 2013), others have reported increased cytokine levels in the periphery and in the brain (Borrell et al., 2002; Garay et al., 2012; Krstic et al., 2012), immune dysregulation (Hsiao et al., 2012), as well as neuropathological features such as activated microglia (Borrell et al., 2002; Krstic et al., 2012 but see Garay et al. 2012) and astrocyte activation (Borrell et al., 2002; Fatemi et al., 2002) in juvenile or adult animals.

Alterations in synaptic structure and function are thought to be central to many neurodevelopmental disorders including ASD and SZ (Marin-Padilla, 1972; Penzes et al., 2011). Neuroanatomical studies from postmortem brains of individuals with neurodevelopmental disorders demonstrate altered number and morphology of dendritic spines, which are the postsynaptic structure of excitatory synapses (Fiala et al., 2002; Hutsler and Zhang, 2010; Penzes et al., 2011). Similarly, synaptic alterations are found in mouse models of these disorders (Comery et al., 1997). Moreover, multiple genetic variations associated with neurodevelopmental disorders are found in genes that have defined roles in synaptic regulation (Grant, 2012; Peca and Feng, 2012). Despite the important role of impaired synaptic development in ASD, *in vivo* analyses of synapse formation and function in MIA offspring are limited (Ito et al., 2010; Elmer et al., 2013). Moreover, it is not known whether the synaptic impairments persist into adulthood and whether they can be ameliorated with early anti-inflammatory treatment.

Here we report that MIA offspring have reduced dendritic spine density and dynamic properties, with impairments persisting into adulthood. We also found an alteration in the interaction between presynaptic boutons and dendritic spines. These structural impairments were accompanied by deficits in excitatory and inhibitory synaptic transmission. Finally, we found that postnatal treatment with an anti-inflammatory drug can prevent the dendritic spine loss as well as the increased marble burying in MIA offspring. We suggest that an altered inflammatory state in the developing brain of MIA offspring affects synaptic development and behavior.

2. Materials and methods

2.1. MIA induction

All protocols were approved by the University of Nebraska Medical Center Institutional Animal Care and Use Committee. YFP-H C57Bl/6J pregnant females were bred at UNMC facility with a 12:12 h light:dark cycle with food and water available *ad libitum*. Mice were mated overnight, and the presence of a vaginal plug on the following morning was noted as embryonic day (*E*)0.5. Pregnant mice were injected intraperitoneally (I.P.) on E12.5 with saline or 20 mg/Kg Poly (I:C) potassium salt (Sigma Aldrich; St. Louis. MO) (Malkova et al., 2012). Pups were allowed to be born naturally. Offspring of saline injected mice are referred to as control offspring and offspring of Poly(I:C) injected mice are referred to as MIA offspring. 3–6 litters from each condition were used for all experiments. With the exception of the behavioral data (where 2–5 mice were used per litter), in all other experiments no more than 1–3 pups were used from each litter. During data collection and analysis the experimenters were blind to the experimental conditions.

2.2. Tissue preparation and immunohistochemistry

Control and MIA offspring were perfused with 4% paraformaldehyde at postnatal day (*P*)17–19, P30 or at 3–4 months. Brain sections (100 microns) containing the somatosensory area were selected for analysis. Sections from P30 and 3–4 months old mice were directly mounted on slides for imaging. Sections from P17–P19 mice were incubated in 10% normal goat serum (NGS) and 0.3% Triton X-100 for 3 min, washed three times with PBS 1×, pre-incubated 1 h in 5% NGS and then immunostained with primary antibodies against GFP (polyclonal 1:300, Life Technologies), VGluT1 (polyclonal 1:300, Millipore), VGluT2 (polyclonal 1:300, Millipore) or GAD-65 (monoclonal 1:100, Developmental Studies Hybridoma Bank) overnight at 4 °C. The secondary antibodies were Alexa 486, 594 and 647 coupled to goat anti-chicken, anti-mouse and anti-guinea pig respectively (1:500, 1:200, 1:500 Invitrogen), in 1% NGS and 0.3% Triton X-100, for 90 min at RT.

2.3. Confocal imaging

Confocal imaging was performed on a Zeiss, LSM 700 using a 40 × 1.4 N.A oil lens. Images were collected in layer 1 of the S1 region at 512 × 512 pixels with pixel size of 0.21 μm and Z step of 0.20 μm, at 8 bit with 488, 555 and 659 nm lasers. Laser power and gain settings were kept constant for all experiments.

2.4. Analysis of spine density, morphology and colocalization with presynaptic markers

For quantitative analysis, a 3-D perspective was rendered by the Surpass module of Imaris software package (Version 6.5, Bitplane, Saint Paul, MN). Dendritic regions analyzed within the ROI were 30–80 μm in length. Spines were classified as stubby, mushroom, thin and filopodia based on a hierarchical algorithm (Kim et al., 2013).

Measurements of VGluT1, VGluT2 and GAD-65 presynaptic puncta were made within a ROI of 25 × 25 × 2 μm in layer 1. Puncta were individually traced in 3D using the Spot Object package of Imaris 6.5 software. All measurements were made within 5–10 microns from the surface of the section to ensure uniformity of antibody penetration. 4–7 ROIs were imaged per mouse.

Qualitative analysis of colocalization between VGluT1/GAD-65 or VGluT2/GAD-65 and dendritic spines was performed on dendrites that were within the immunostained volume and on the same filament previously selected for the density of spines, using the ImarisColoc software. After background subtraction, the threshold value for each channel was automatically adjusted, following an algorithm previously described (Costes et al., 2004). The colocalized voxels representing presynaptic puncta on spines were manually counted and reported as percent of spines with a colocalized puncta. The dendritic parameters (length, width and number of spines counted) for the various experiments are included in Supplemental Table 1.

2.5. Analysis of surface MHCI proteins

Surface MHCI (sMHCI) staining was performed on fixed brain sections (100 microns) without permeabilization. Brain section were incubated with monoclonal mouse antibody to MHCI (1:250, OX-18, Serotec) together with a VGluT1 antibody (polyclonal 1:300, Millipore) in 5% NGS without Triton X-100 overnight at 4 °C, then washed three time in PBS 1×, incubated them with Alexa 486 and 647 (1:500 and 1:300 respectively) for 90 min and mounted on slides. Measurements of sMHCI were made within a ROI of 10 × 10 × 2 μm in layer 1. In order to ensure that only surface MHCI was measured rather than intracellular protein exposed due to the mechanical damage to the surface of the brain section, we used exclusion of VGluT1 staining (intracellular protein) to determine where in the *Z*-axis of a confocal stack to measure sMHCI (Supplemental Fig. 3). Puncta were then individually traced in 3D using the Spot Object package of Imaris 6.5 software.

2.6. In vivo two-photon imaging

Thinned-skull cranial windows were prepared above the somatosensory cortex in a single hemisphere of YFP-H C57Bl6/J mice between P17 and P19 as previously described (Padmashri et al., 2013). Imaging was performed with a multiphoton microscope (Moving Objective Microscope (MOM), Sutter), using a Ti:sapphire laser (Chameleon Vision II, Coherent) tuned to 925 nm. Images were collected with a Nikon water immersion objective (60×, 1.0 NA). For imaging, we used ScanImage software (Pologruto et al., 2003) written in MATLAB (MathWorks). During an imaging session, five to six regions of interest (ROIs) per animal were selected along the dendritic tufts of YFP-expressing layer 5 pyramidal neurons and imaged at intervals of 12 min sequentially. Each ROI consisted of a stack of images (20–40 optical sections, separated axially by 1 µm). Each optical section was collected at 512 × 512 pixels, 0.15 µm/pixel.

2.7. Analysis of spine dynamics

Dendritic spine analysis was performed using ImageJ software. Dendritic segments, 20–60 µm in length, were identified in three-dimensional image stacks taken at different time points, and all spines that clearly protruded from the shaft (>0.5 microns) were marked. The rates of spines gained and lost were defined, respectively, as the fraction of spines that appeared and disappeared between two successive frames, relative to the total spine number. Spine turnover rate (TOR) was defined as the sum of the spines lost and gained divided by twice the total number (Holtmaat et al., 2005).

2.8. Slice electrophysiology

Coronal slices containing the S1 area were obtained from P17–P19 old control and MIA offspring as previously described (Padmashri et al., 2013). For recording, slices were superfused in a submersion type recording chamber at room temperature (22–24 °C) with artificial cerebrospinal fluid (ACSF) saturated with 95% O_2/5% CO_2. Somatic whole-cell recordings were obtained from upper layer 2 pyramidal cells of S1 visualized with infrared differential interference contrast optics. Recordings were performed using an Axoclamp-2B amplifier (Axon Instruments), signals were filtered at 3 kHz, digitized (Digidata 1322A; Molecular Devices), and sampled at 10 kHz using pClamp 9.0 (Molecular Devices). Data was analyzed offline using Mini-Analysis software (Synaptosoft). mEPSCs and mIPSCs were recorded at –70 mV. For mEPSC recordings, ACSF contained 1 µm TTX (Tocris) and 10 µm bicuculline methiodide (Sigma). For mIPSCs recordings, ACSF contained 1 µm TTX, 20 µm NBQX and 50 µm AP-5. For analysis of mEPSCs, 5 min of recording was used. Analysis of mIPSCs was done on data recorded for 2 min.

2.9. Marble burying

Marble burying is a widely used test of repetitive and perseverative behaviors (Thomas et al., 2009). It was performed on 2 months old male and female mice. Following acclimatization, 30 glass marbles were lightly placed on thick bedding at a 5 × 6 arrangement. Individual mice were placed in the cage with the lid closed for 30 min. The mouse was then removed and marbles were scored. A marble was considered buried if 2/3 of it was covered by bedding. The observer was blinded to the experimental conditions.

2.10. Drug administration

Ibudilast (Sigma) was dissolved in corn oil at 5 mg/ml and administered to lactating dams with an Intraperitoneal (IP) injection daily for 2 weeks (starting 24 h post parturition) at a dose of 30 mg/Kg. This manner of administration was chosen in order to not stress the pups with daily IP injections or gavaging. Control dams received an equal dose of vehicle (corn oil) throughout the treatment period. Mice were either sacrificed at P17 or weaned at postnatal day 30, and were group housed with females and males in separate cages.

2.11. Statistical analysis

Data are reported as mean ± s.e.m. For all analysis, with the exception of Supplemental Figs. 1, 5 and 6, we used n = animals. Normal distribution was tested using Kolmogorov–Smirnov test and variance was compared. Analysis was done either using two-sided unpaired Student's t-test, multiple t-test with the Sidak–Bonferroni correction, one-way ANOVA or two-way ANOVA with the Bonferroni method for *post hoc* multiple comparisons. In two-way ANOVA if interaction was not significant a *post hoc* test was not conducted. Data was analyzed using the Graph Pad Prism software.

3. Results

3.1. Reduced dendritic spine density in MIA offspring

Altered synaptic structure is associated with several neurodevelopmental disorders including ASD and has been demonstrated in genetic mouse models for these disorders. Previous studies have shown that there is a reduction in the number of excitatory synapses in dissociated cortical neurons from MIA offspring (Elmer et al., 2013), but whether synaptic impairments are observed *in vivo* is not known. We therefore first investigated if we can detect altered density of dendritic spines, postsynaptic sites of excitatory synapses, in the cortex of MIA offspring *in vivo*. Pregnant YFP-H mice were injected at E12.5 with 20 mg/Kg Poly (I:C) (MIA) or saline (control). In these mice a subset of layer 5 pyramidal neurons are expressing YFP (Feng et al., 2000), allowing us to analyze spine density in the control and MIA offspring mice (Fig. 1a and b). At P17–19 we found a 23% reduction in the density of dendritic spines on layer 1 apical dendrites (Fig. 1c, P = 0.018). A similar effect with a 16% reduction in spine density was found in the basal dendrites of P30 mice of MIA offspring (Suppl. Fig. 1, P = 0.004). These results indicate that in developing and adolescent mice, maternal immune activation leads to reduced density of cortical dendritic spines.

We next asked if spine morphology was altered in MIA offspring. We categorized spines on apical dendrites as mushroom, thin, stubby or filopodia. We found that in the MIA offspring at P17–19 there was a general decrease in all spine categories (Fig. 1d).

3.2. Impaired dynamics of dendritic spines in vivo

During development dendritic spines are highly dynamic structures with spines appearing and disappearing on a time scale of minutes (Dunaevsky et al., 1999). Dendritic spine motility is thought to facilitate contacts with axons and mediate the formation of proper neuronal circuitry. Impairments in spine dynamics have been demonstrated in several mouse models of neurodevelopmental disorders. We therefore used transcranial *in vivo* two-photon laser scanning time-lapse microscopy to measure dendritic spine dynamics in intact

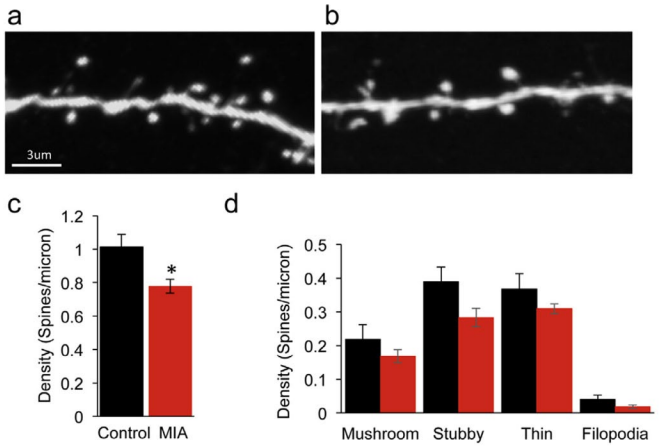

Fig. 1. Reduced cortical dendritic spine density in young MIA offspring. Confocal images of layer 5 pyramidal neuron apical tuft dendrites from P17 offspring of control (a) and MIA (b) YFP-H mice. (c) MIA results in a reduction in total dendritic spine density (control: 1.014 ± 0.07 spines/micron, n = 4; MIA: 0.78 ± 0.04 spines/ micron, n = 6, P = 0.018, unpaired t-test). (d) MIA results in a general reduction in density of all dendritic spine categories although these differences did not reach significance following multiple comparison corrections (mushroom P = 0.27, stubby P = 0.06, thin P = 0.185 and filopodia P = 0.11, multiple t-test with Sidak–Bonferroni correction. Data are represented as mean ± SEM.

cortical circuits (Fig. 2a and b). We first confirmed that in this separate cohort of mice with spines observed *in vivo* through a thinned skull window the density of spines was reduced in the MIA offspring by 22% (Fig. 2c, P = 0.0001).

We next analyzed the time-lapse images to measure the dynamic properties of spines (Fig. 2a and b). We found that dendritic spines in MIA offspring were dramatically less dynamic than in control mice with a 37% decrease in the turnover rate (TOR) of spines (Fig. 2d, P = 0.013). The reduction in TOR was due to both lower rate of spine gain (Fig. 2e, P < 0.0001) and reduced rate of spine loss (Fig. 2f, P = 0.028). These findings demonstrate that in MIA offspring there is impairment in density, morphology and dynamics properties of dendritic spines.

3.3. Altered excitatory and inhibitory presynaptic input in the cortex of MIA offspring

To determine if the altered number, shape and dynamic properties of spines are accompanied by alterations in presynaptic inputs, we performed a quantitative analysis of excitatory and inhibitory presynaptic puncta using the markers VGluT1, VGluT2 and GAD-65 respectively (Fig. 3a and b and Suppl. Fig. 2). We found no difference in the number or size of VGluT1, VGluT2 or GAD-65 puncta in the cortex of MIA offspring (Fig. 3c and d). To determine if the synaptic inputs reorganized on the remaining dendritic spines in MIA offspring we analyzed the colocalization between the YFP labeled dendrites and the three synaptic markers (Fig. 3e–f). Although dendritic spines are the predominant sites of excitatory synaptic input, recent studies demonstrate that inhibitory inputs on dendritic spines are more prevalent than previously appreciated (Chen et al., 2012). We therefore analyzed the proportion of dendritic spines contacted by the excitatory and inhibitory synaptic puncta. We saw a trend towards increase in the proportion of spines contacted by VGluT1 or GAD-65 puncta in the MIA offspring (Fig. 3h, P = 0.048 and P = 0.024 respectively) and no change in spines contacted by VGluT2 (P = 0.78). These results suggest that while spine density is reduced the persisting spines are more likely to be contacted by both excitatory and inhibitory presynaptic puncta (Fig. 3h) which is consistent with no discernable change in total number of presynaptic puncta (Fig. 3c). Strikingly, in MIA offspring we also found a 103% increase in spines that were doubly innervated and contacted by both VGluT1 and GAD-65 puncta (Fig. 3h, P = 0.003). In summary these data indicate that in MIA offspring, there is not only a decrease in total number of excitatory synapses but also a dramatic change in the number of dendritic spines that receive multiple synaptic inputs likely resulting in altered processing of incoming synaptic inputs.

3.4. Impaired excitatory and inhibitory synaptic function in MIA offspring

We next examined how MIA affects synaptic function in the cortex. We performed whole-cell voltage-clamp recordings from layer 2 pyramidal neurons in the somatosensory cortex. While we found a 26% decrease (P = 0.007) in the frequency of miniature excitatory postsynaptic currents (mESPC), no difference (P = 0.097) was observed in the amplitude of mEPSC in the MIA offspring (Fig. 4a and b). These data are consistent with reduced density of dendritic spines in the MIA offspring.

We have also observed altered inhibitory synaptic transmission in the MIA offspring (Fig. 4c and d). Although there was no difference (P = 0.226) in miniature inhibitory postsynaptic current (mIPSC) frequency, mIPSC amplitude increased by 16% (P = 0.046). Thus MIA offspring exhibit both structural and functional impairments in excitatory and inhibitory synaptic transmission.

3.5. Dendritic spine impairments in MIA offspring can be prevented by an anti-inflammatory drug treatment

Previous studies documented altered expression in the level of cytokines in the brains of the MIA mouse offspring (Garay et al., 2012). Cytokines regulate the levels of MHCI, a negative regulator of synapse formation (Glynn et al., 2011) that is increased in neurons from MIA offspring (Elmer et al., 2013). We therefore predicted that a reduction in an inflammatory state in the MIA offspring during development would ameliorate the synaptic deficits. To test this hypothesis we treated control and MIA offspring with an anti-inflammatory drug ibudilast during the first 2 postnatal weeks. Ibudilast is a type IV-phosphodiesterase inhibitor that modulates the activity of glial cells such as the microglia and astrocytes, suppressing the production of proinflammatory cytokines (Suzumura et al., 1999; Mizuno et al., 2004; Ledeboer et al., 2006). Ibudilast, long used for treatment of asthma, can cross the blood brain barrier and in humans can be found in breast milk (Web reference: Kyorin Pharmaceuticals; http://www.kyorin-pharm.co.jp/prodinfo/medicine/pdf/KETAS_Capsules.pdf). Lactating control and MIA dams were injected with 30 mg/Kg ibudilast or vehicle daily for 2 weeks starting 1 day after parturition. We have determined that ibudilast can be detected in serum and brains of offspring whose lactating mothers received a daily injection of ibudilast (Supplemental Fig. 4). At P17 the density of dendritic spines on apical dendritic tufts in layer 1 of the somatosensory cortex was determined. As expected, MIA offspring treated with vehicle had a 17% reduction (P = 0.026) in spine density as compared to control mice (Fig. 5a and b). Importantly, treatment of MIA offspring with ibudilast resulted in prevention of dendritic spine loss (P = 0.007) while having no effect on spine density in control mice (P > 0.9). We also tested if an increase in surface MHC class I proteins (sMHCI) can be detected *in vivo* in MIA offspring and if it can be prevented by ibudilast treatment. As has previously been shown

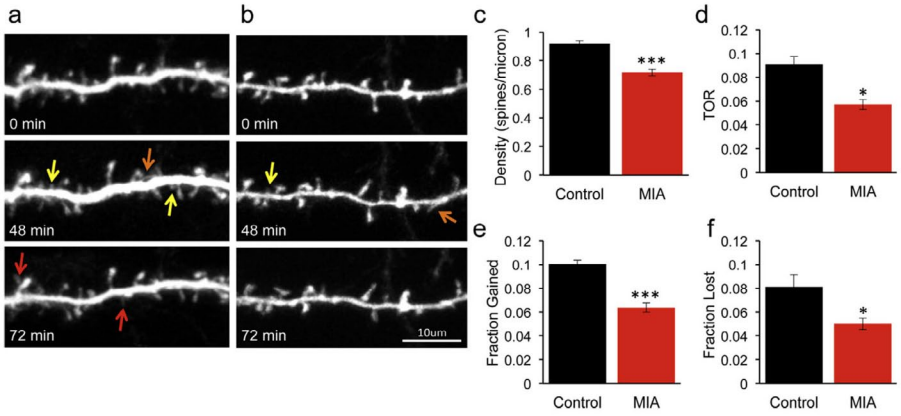

Fig. 2. Reduced density and dynamics of dendritic spines in MIA offspring. Multiphoton imaging of cortical neurons from P17 YFP-H mice through a thinned skull window in control (a) and MIA (b) offspring. Images were collected every 12 min for a period of 1.5 h. Note the reduced density of dendritic protrusions in the MIA offspring. Dendritic spine formation (red arrows) and elimination (yellow arrows) is prevalent in control but not MIA offspring. Spines that appear but then disappear are marked with an orange arrow. (c–f) Quantification of spine parameters imaged *in vivo* in 5 mice for each condition (multiple *t*-tests with Bonferroni corrections). Spine density is reduced in MIA offspring (control: 0.92 ± 0.02 spines/micron; MIA: 0.72 ± 0.02 spines/micron, $P = 0.0001$). Turnover rate (TOR) is reduced in MIA offspring (control: 0.091 ± 0.01; MIA 0.057 ± 0.004, $P = 0.013$) due to reduction in both fraction of spines gained (control: 0.1 ± 0.003; MIA: 0.064 ± 0.004, $P < 0.0001$) and fraction of spines lost (control: 0.08 ± 0.01; MIA: 0.05 ± 0.005, $P = 0.028$). Data are represented as mean ± SEM.

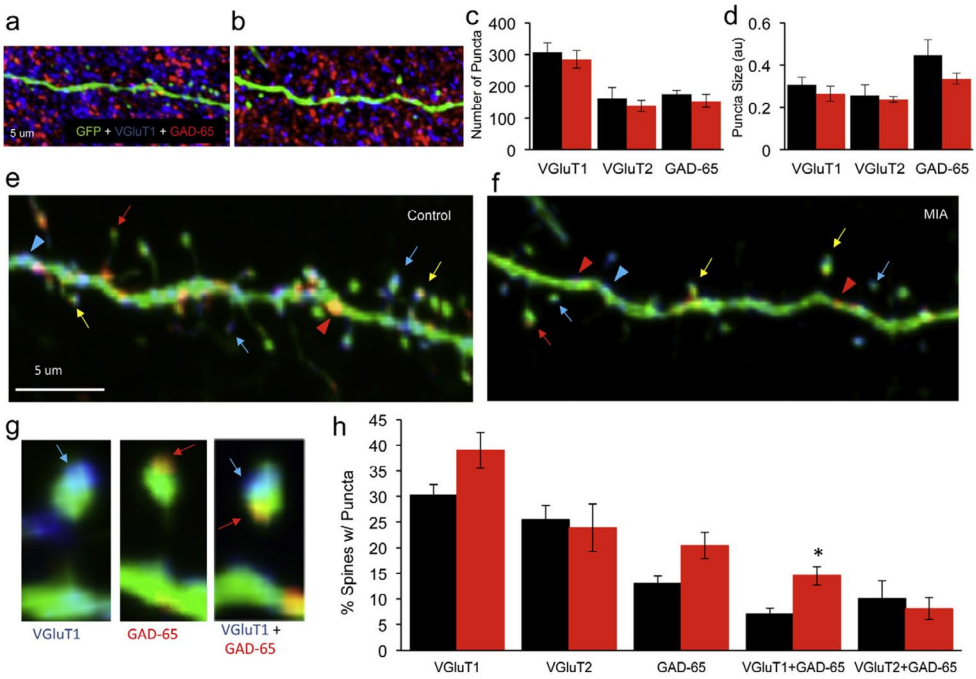

Fig. 3. Altered presynaptic input in the cortex of MIA offspring. (a and b) Cortical P17 sections from YFP-H mice immunostained with VGluT1 (blue) and GAD-65 (red) in control (a) and MIA offspring (b). (c and d) Quantification of VGluT1, VGluT2 and GAD-65 puncta do not show a reduction in number of puncta in MIA offspring. VGluT1, control (black): 307 ± 29.57, $n = 8$; MIA (red): 285.3 ± 28.15, $n = 8$, $P = 0.60$; VGluT2, control: 162.5 ± 32.54, $n = 8$; MIA: 138.3 ± 18.56, $n = 6$, $P = 0.57$; GAD-65, control: 174.5 ± 12.7, $n = 8$; MIA: 154.2 ± 20.56, $n = 8$, $P = 0.41$). No significant difference in the volume of the puncta was observed. VGluT1, control: 0.305 ± 0.04, $n = 6$; MIA: 0.264 ± 0.035, $n = 8$, $P = 0.46$; VGluT2, control: 0.258 ± 0.048, $n = 8$; MIA: 0.239 ± 0.012, $n = 6$, $P = 0.75$; GAD-65, control: 0.448 ± 0.073, $n = 6$; MIA: 0.336 ± 0.027, $n = 8$, $P = 0.13$ unpaired *t*-test). (e and f) Colocalization analysis of VGluT1 and GAD-65 with YFP labeled apical tuft dendrites and spines shown in (a) and (b). Arrowheads and arrows denote colocalization of a punctum with a dendritic shaft or spine respectively. Red and blue arrows mark colocalization with GAD-65 and VGluT1 puncta respectively. A yellow arrow marks a dendritic spine in a putative contact with both GAD-65 and VGluT1 puncta. (g) High magnification images of colocalization of presynaptic puncta on dendritic spines showing examples of spines with VGluT1, GAD-65 and VGluT1 + GAD-65 puncta. (h) Quantification of percent spines contacted by puncta. A non-significant increase in spines contacted by VGluT1, VGluT2 or GAD-65 in the MIA offspring (VGluT1, control: 30.24 ± 2.1%, $n = 9$; MIA: 39 ± 3.5%, $n = 9$, $P = 0.048$; VGluT2, control: 25.46 ± 2.84%, $n = 6$; MIA: 23.92 ± 4.66%, $n = 6$, $P = 0.78$ and GAD-65, control: 13.02 ± 1.47%, $n = 11$, MIA: 20.4 ± 2.56%, $n = 12$, $P = 0.024$). Quantification of percent of dendritic spines in putative contact with both VGluT1 and a GAD-65 puncta demonstrates an increase in MIA offspring (control: 7.15 ± 1.1%, $n = 9$; MIA: 14.53 ± 1.78%, $n = 9$, $P = 0.003$). Multiple *t*-tests with Sidak–Bonferroni corrections were used and only the VGluT1 + GAD category survived the correction. Data are represented as mean ± SEM.

in cultured neurons from MIA offspring (Elmer et al., 2013), we found a 37% increase ($P = 0.01$) in sMHCI staining in cortical sections from vehicle treated MIA (Fig. 6a and b). Although there was a 17% reduction in the expression of sMHCI in ibudilast treated MIA offspring, this trend was not significant ($P = 0.16$). We therefore conclude that postnatal anti-inflammatory treatment can prevent spine loss in MIA offspring but this is only partially mediated by reduction in sMHCI protein expression.

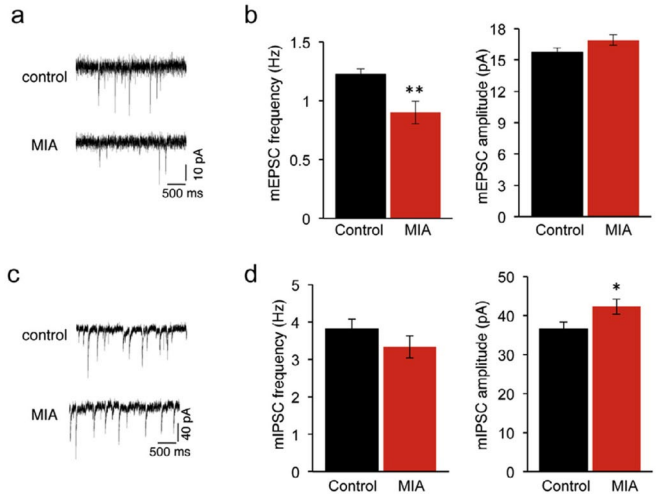

Fig. 4. Altered cortical excitatory and inhibitory synaptic transmission in the MIA offspring. (a) mEPSCs recorded from layer 2 pyramidal neurons in somatosensory cortex from control and MIA offspring. (b) Reduced mEPSCs frequency (control (black): 1.22 ± 0.05 Hz, *n* = 9 mice, 28 cells; MIA (red): 0.90 ± 0.1 Hz, *n* = 8 mice, 32 cells, *P* = 0.007) with no difference in the amplitude of mEPSC (control: 15.72 ± 0.44 pA, MIA: 16.91 ± 0.51 pA, *P* = 0.097) was observed in the MIA offspring. (c) mIPSCs recorded from layer 2 pyramidal neurons in somatosensory cortex from control and MIA offspring. (d) No difference in mIPSCs frequency (control: 3.82 ± 0.26 Hz, *n* = 12 mice, 41 cells; MIA: 3.33 ± 0.29 Hz, *n* = 9 mice, 35 cells, *P* = 0.226) and increased mIPSC amplitude (control: 36.51 ± 1.82 pA, MIA: 42.25 ± 1.93 pA, *P* = 0.046) was observed in MIA offspring. Data are represented as mean ± SEM.

3.6. Dendritic spine impairments in MIA offspring persist into adulthood

We next examined if spine loss persists in adult MIA offspring and if a 2-week postnatal treatment is sufficient to normalize spine densities in the adult mice. Lactating dams were treated with 30 mg/Kg ibudilast for 2 weeks after birth and at 3 months of age the density of dendritic spines on apical dendritic tufts in layer 1 of the somatosensory cortex was determined. We found that the dendritic spine deficit observed at P17 is maintained into adulthood. There was a 32% decrease (*P* = 0.04) in the density of dendritic spines in the 3 months old vehicle treated MIA offspring as compared to the vehicle treated control offspring (Fig. 7a and b). Although we observed a substantial reversal of dendritic spine density impairment in MIA offspring whose mothers received a daily injection of ibudilast for the first two postnatal weeks (Fig. 7a and b) this result did not reach significance (*P* = 0.26) unless images rather than mice were considered as *N* (Suppl. Fig. 5). The control offspring, whose mothers were treated with the ibudilast, did not present any changes (*P* > 0.9) in density of spines (Fig. 7a and b). These data indicate that spine deficits persist into adulthood in MIA offspring but anti-inflammatory treatment during the first two postnatal weeks is not sufficient for the spine improvements to persist into adulthood.

3.7. Anti-inflammatory drug, ibudilast, prevents increased marble burying behavior in MIA offspring

MIA offspring exhibit impairments in several ASD and SZ relevant behaviors (Malkova et al., 2012). Marble burying is an assay used to test for repetitive and perseverative behaviors (Thomas et al., 2009). Previous studies demonstrated that MIA offspring of the same strain exhibit increased marble burying (Malkova et al., 2012). We therefore tested if treatment with ibudilast can reduce marble burying in MIA offspring using the same cohort of mice used for the spine analysis above. At postnatal day 60, MIA offspring treated with vehicle buried 42% more marbles as compared to control mice treated with vehicle (Fig. 7c, main effect of prenatal treatment *P* = 0.0001). We found that treatment of MIA offspring with ibudilast during the first 2 postnatal weeks normalized the marble burying behavior (Fig. 7c, main effect of ibudilast treatment, *P* = 0.0003). Similar results were observed when mice from the same litter were averaged (Suppl. Fig. 6). These findings suggest that prenatal immune activation generally increased marble burying, whereas ibudilast treatment generally reduced it.

We next wanted to determine if there was a relationship between cortical spine density and marble burying. For a subset of mice we had both the marble burying activity at P60 and the subsequent recorded spine density data at 3 months. We found an inverse correlation between dendritic spine density and marble burying (Fig. 7d, *r* = –0.49, *P* = 0.048). These data suggest that there is a link between cortical spine density and the marble burying deficit in the MIA offspring.

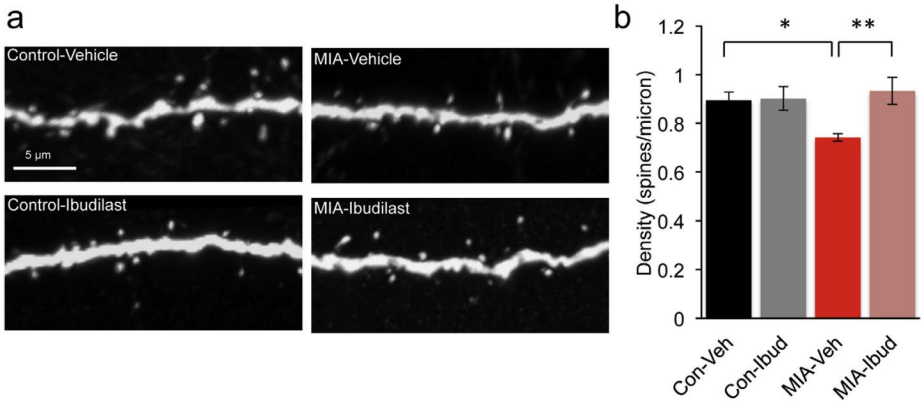

Fig. 5. Postnatal treatment with an anti-inflammatory drug ibudilast, prevents spine loss in young mice. (a) Layer 5 pyramidal neuron apical tuft dendrites from P17 control + vehicle, control + ibudilast, MIA + vehicle and MIA + ibudilast offspring mice treated during the first 2 postnatal weeks. (b) Two-way ANOVA was first used to test for the presence of interaction between drug treatment and experimental groups. This revealed an interaction consistent with the observation that ibudilast increased dendritic spine density in the MIA offspring but had no effect on the controls $F(1, 20) = 6.296$, $P = 0.021$. *Post hoc* two-way ANOVA with Bonferroni's correction confirm a reduction in spine density in MIA + vehicle offspring (control + vehicle: 0.89 ± 0.03 spines/micron, *n* = 6 mice; MIA + vehicle: 0.74 ± 0.01 spines/micron, *n* = 8, mice, *P* = 0.026) and that reduction is prevented by postnatal treatment with the anti-inflammatory drug ibudilast (MIA + ibudilast: 0.93 ± 0.05 spines/micron, *n* = 5 mice, MIA + vehicle: 0.74 ± 0.01 spines/micron, *n* = 8 mice, *P* = 0.007). No change in spine density in control + ibudilast offspring (control + vehicle: 0.89 ± 0.03 spines/micron, *n* = 6 mice; control + ibudilast: 0.90 ± 0.05 spines/micron, *n* = 5 mice, *P* > 0.9).

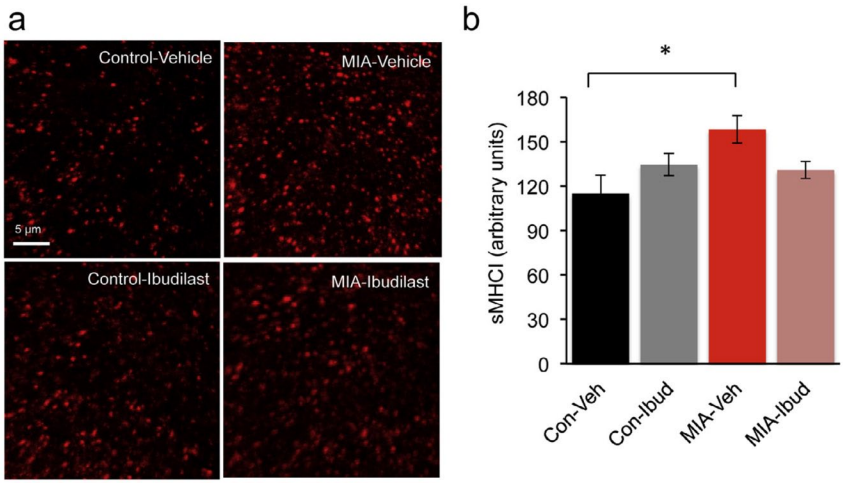

Fig. 6. Surface MHCI proteins are increased *in vivo* in MIA offspring. (a) Representative confocal images of cortical P17 control + vehicle, control + ibudilast, MIA + vehicle and MIA + ibudilast offspring, immunostained for sMHCI. (b) Quantification of surface MHCI. Two-way ANOVA was first used to test for the presence of interaction between drug treatment and experimental groups. This revealed an interaction consistent with the observation that ibudilast decreased sMHCI in the MIA offspring but had no effect on the controls ($F(1, 28) = 6.779$, $P = 0.015$). *Post hoc* two-way ANOVA with Bonferroni's correction confirms an increase in sMHCI in MIA + vehicle offspring (control + vehicle: 115 ± 12.2 a.u., $n = 8$; MIA + vehicle: 158.3 ± 9.3 a.u., $n = 8$, $P = 0.01$) but the increase is not completely prevented by the postnatal treatment with ibudilast (MIA + ibudilast: 130.9 ± 5.7 a.u., $n = 8$, MIA + vehicle: 158.3 ± 9.3 a.u., $n = 8$, $P = 0.16$).

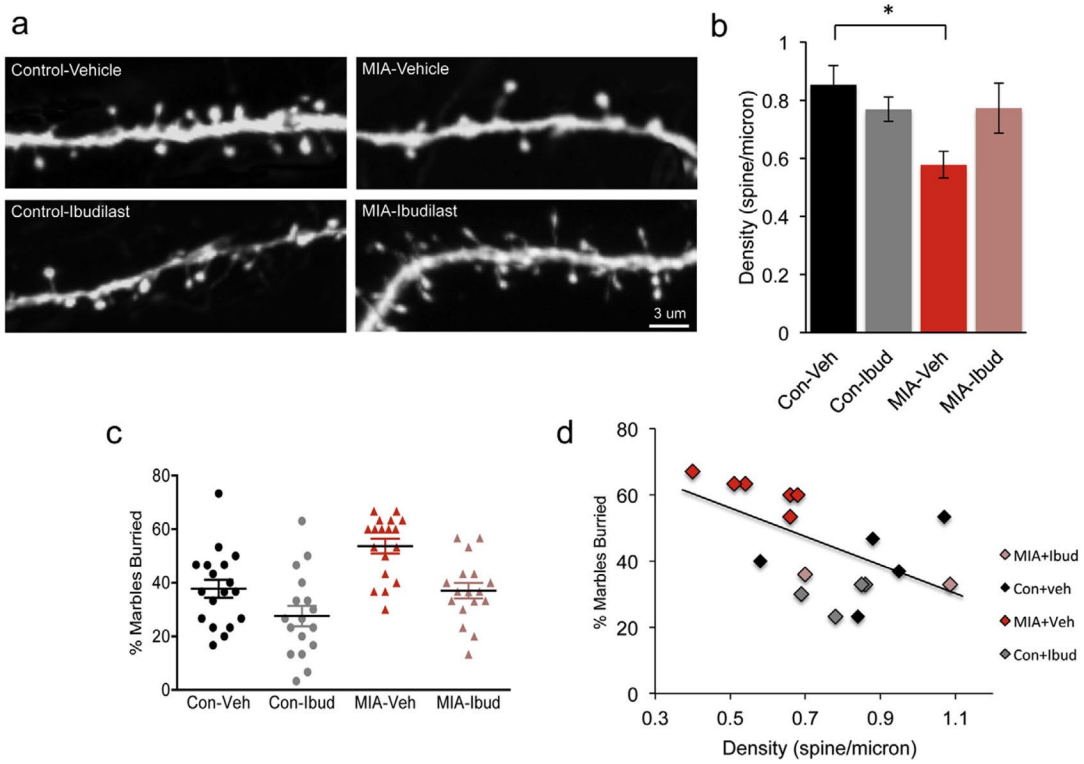

Fig. 7. Dendritic spine impairments in MIA offspring persist into adulthood and are correlated with increased marble burying. (a) Layer 5 pyramidal neuron apical tuft dendrites from 3 month old control + vehicle, control + ibudilast, MIA + vehicle and MIA + ibudilast offspring mice treated during the first 2 postnatal weeks. (b) Two-way ANOVA was first used to test for the presence of interaction between drug treatment and experimental groups. This revealed an interaction consistent with the observation that ibudilast increased dendritic spine density in the MIA offspring but had no effect on the controls $F(1, 19) = 4.62$, $P = 0.04$. *Post hoc* two-way ANOVA with Bonferroni's correction indicates that a reduction in spine density in MIA + vehicle offspring persists into adulthood (control + vehicle: 0.85 ± 0.07 spines/micron, $n = 6$ mice; MIA + vehicle: 0.58 ± 0.05 spines/micron, $n = 6$ mice, $P = 0.04$) but is not prevented by postnatal treatment with the anti-inflammatory drug ibudilast (MIA + ibudilast: 0.77 ± 0.09 spines/micron, $n = 6$ mice, MIA + vehicle: 0.58 ± 0.05 spines/micron, $n = 6$ mice, $P = 0.25$). No changes in spines density in control + ibudilast offspring (control + vehicle: 0.85 ± 0.07 spines/micron, $n = 6$ mice; control + ibudilast: 0.77 ± 0.04 spines/micron, $n = 5$ mice, $P > 0.9$). (c) Marble burying is increased in MIA offspring and this increase is prevented by postnatal ibudilast treatment. There was a main effect of prenatal treatment, $F(1,67) = 16.99$, $P = 0.0001$, as well as a main effect of drug treatment, $F(1,67) = 14.37$, $P = 0.0003$ on marble burying but no significant interaction $F(1,67) = 0.5$, $P = 0.48$. Marble burying increased in MIA offspring (control + veh: 37.7 ± 3.3%, $n = 18$ mice from 4 litters; MIA + veh: 53.7 ± 2.7%, $n = 18$ mice from 4 litters). This increase is reduced in MIA offspring treated with ibudilast during the first 2 postnatal weeks (MIA + Ibud: 37 ± 2.9%, $n = 17$ from 4 litters). There was also a mild effect of ibudilast on control offspring (control + Ibud: 27.6 ± 3.8%, $n = 17$ from 4 litters). (d) The spine density observed at 3 months is inversely correlated with the percent of marbles buried at P60 (Pearson $r = \_0.49$, $n = 18$, $P = 0.048$). Data are represented as mean ± SEM.

4. Discussion

Here we show that MIA offspring, an environmental risk factor for ASD and SZ, exhibit impairments in cortical dendritic spine morphogenesis and motility *in vivo* with reduced spine density persisting into adulthood. The excitatory and inhibitory connectivity on the dendritic spines is altered in the MIA offspring. Functionally, layer 2 pyramidal neurons receive fewer excitatory synaptic inputs of similar strength as well as similar number of inhibitory synaptic inputs with increased efficacy in the MIA offspring as in control mice. Finally, postnatal treatment of MIA offspring with an anti-inflammatory drug ibudilast can ameliorate the spine impairments observed in young mice as well as alteration in an ASD relevant behavior, increased marble burying. These data suggest that increased inflammatory state during early postnatal weeks is responsible for altered synaptic connectivity and impaired behavior and that early anti-inflammatory treatment can have an ameliorating effect on both synapses and behavior.

Although impairments in dendritic spines are a hallmark of many neurodevelopmental disorders (Penzes et al., 2011), dendritic spines have never been analyzed in MIA offspring. Here we report that MIA offspring have a significantly reduced number of dendritic spines an impairment that persists into adulthood and therefore could be contributing to behavioral deficits observed in adult mice. Reduced number and immature appearing dendritic spines have been reported in postmortem SZ brain (Selemon and Goldman-Rakic, 1999; Glantz and Lewis, 2000) as well as mouse models for SZ (Lee et al., 2011). Although reduced spine density has been reported in a MECP2 mutant ASD mouse model (Landi et al., 2011; Jiang et al., 2013) it is less consistent with most ASD related spine pathophysiology where increase in spine density is more prevalent (Hutsler and Zhang, 2010; Penzes et al., 2011).

During development, dendritic spines are highly dynamic structures with new spines forming and others disappearing on a time scale of minutes (Dailey and Smith, 1996; Dunaevsky et al., 1999). While spine motility substantially wanes in adult mice (Dunaevsky et al., 1999; Grutzendler et al., 2002; Holtmaat et al., 2005; Cruz-Martin et al., 2010) it is regulated by sensory experience (Trachtenberg et al., 2002) and learning (Xu et al., 2009). Abnormal dendritic spine turnover rates have been reported in other mouse models of neurodevelopmental disorders such as Fragile X syndrome (Cruz-Martin et al., 2010; Pan et al., 2010; Padmashri et al., 2013) and Rett syndrome (Landi et al., 2011). Unlike the fmr1 KO (Cruz-Martin et al., 2010; Pan et al., 2010; Padmashri et al., 2013) and similar to Rett mouse model (Landi et al., 2011) in MIA offspring the turnover rate of dendritic spine dynamics is substantially reduced, with both formation and elimination of spines being affected. Dendritic spine dynamics is thought to facilitate formation of contacts with axons and to be necessary for formation of proper circuitry. It is possible that the reduced spine dynamics in MIA offspring impairs the ability of neurons to modify connectivity in response to experience.

In addition to the postsynaptic changes we analyzed the presynaptic terminals and their interaction with dendrites and spines. We found no overall change in the total number of excitatory presynaptic puncta labeled with VGluT1 or VGluT2 in the P17 MIA cortex. Together with the spine density reduction our findings are consistent with previous reports of reduced number of excitatory synapses in neuronal cultures isolated from MIA brains (Elmer et al., 2013). Based on our counts of spines contacted by VGluT1 and VGluT2 puncta we estimate that maximally 55% of spines are contacted by an excitatory synapse. Although this might seem low one needs to keep in mind that at P17 many dendritic spines are transient and these have been shown to typically not to be in contact with excitatory presynaptic terminals (Knott et al., 2006). We found that MIA results in reorganization of synapses on dendrites; the proportion of spines contacted by VGluT1 but not VGluT2 increases in MIA offspring. While VGluT1 containing terminals are intracortical in origin, majority of VGluT2 terminals are of thalamic origin (Hur and Zaborszky, 2005). Differential regulation of VGluT1 and VGluT2 by activity has been previously reported (De Gois et al., 2005) and our results suggest circuit specific susceptibility to MIA. It is possible that with fewer spines available, axons contact previously uninnervated spines as well as place a second bouton on an existing synapse. The increase in the proportion of VGluT1 innervated spines in MIA offspring is consistent with the observed increased spine stability (Knott et al., 2006). We also observed a sizable proportion of spines that are dually innervated by excitatory and inhibitory presynaptic boutons, which doubled in MIA offspring. Previous studies have shown that such dually innervated spines are particularly prominent on the apical dendrites in layer 1 and predominantly involve VGluT2 containing terminals in the adult (Kubota et al., 2007). It is possible that during development the prevalence of VGluT1 terminals that co-innervate a dendritic spine together with an inhibitory synapse is higher than in the adults. Although in this study dendritic spines together with presynaptic terminals were not imaged dynamically, it is has been reported that spines innervated by both excitatory and inhibitory synapses are more stable than singly innervated spines (Chen et al., 2012; Chen and Nedivi, 2013), consistent with reduced turnover rate of spines observed in our study. Importantly, our study indicate that both pre- and postsynaptic structures are altered in MIA offspring and are likely to lead to altered neuronal processing.

Consistent with structural synaptic alterations, we found altered synaptic transmission in the MIA cortex. The reduction in spine density is consistent with reduced mEPSC frequency. Although the lack of change in mIPSC frequency was consistent with a similar number of GAD-65 puncta in layer 1, we did not detect an anatomical correlate to the increase in mIPSC amplitude recorded from layer 2 pyramidal neurons. Synaptic transmission alterations in MIA offspring have also been previously measured in the hippocampus where reduced excitatory but not inhibitory synaptic transmission has been reported (Ito et al., 2010). The lack of complete electrophysiological correlates in our study could be explained by cell and layer specific differences as has been previously shown (Dickerson et al., 2014). It is also possible that a change in inhibitory synapses that converge on cell bodies of neurons (rather than on distal dendrites) more directly reflects the electrophysiology recordings. Interestingly, increased $GABA_A$ receptors were found on soma and axon initial segment of pyramidal neurons in the prefrontal cortex of SZ patients (Volk et al., 2002). Our findings of reduced excitatory synaptic transmission are consistent with the reduction in synaptic proteins and dendritic spines found in SZ brains (Garey et al., 1998; Glantz and Lewis, 2000; Harrison and Eastwood, 2001). Alterations in ratio of excitation/inhibition are also found in ASD (Zikopoulos and Barbas, 2013) but the specific disruption depends on the mutation, cell type and the synapse studied (Dani et al., 2005; Tropea et al., 2009; Olmos-Serrano et al., 2010; Wallace et al., 2012).

Altered expression of cytokines and markers of oxidative stress, as well as presence of activated astrocytes and microglia, have been reported in ASD and SZ brains and suggest that potentially chronic neuroinflammatory state can contribute the symptoms and pathology of these disorders (Patterson, 2011). The degree to which a pro-inflammatory profile can be observed systemically and in the brains of MIA offspring is still debated, yet alterations in levels of cytokines have been observed in fetal (Meyer et al., 2006), postnatal and adult brain of MIA offspring (Garay et al., 2012; Krstic et al., 2012) as well as altered number of activated microglia and astrocytes (Borrell et al.,

2002; Krstic et al., 2012). We therefore asked if reducing the inflammatory state during early development could ameliorate the synaptic and behavioral impairments. To investigate this possibility, we tested the impact of the anti-inflammatory drug ibudilast, a phosphodiesterase inhibitor that modulates the activity of glial cells microglia and astrocytes, suppressing the production of proinflammatory cytokines (Ledeboer et al., 2006). While studies have shown the potential of ibudilast in reducing neuroinflammation in a number of neurological conditions such as relapsing-remitting multiple sclerosis, neuropathic pain and drug abuse (Rolan et al., 2009; Snider et al., 2013), there are currently no studies that document evidence in ASD. We observed that administration of ibudilast during the first 2 postnatal weeks through the lactating dam prevented dendritic spine impairments in young MIA offspring as well as the increased marble burying activity at 2 months. It would be interesting to determine if longer postnatal treatment would result in persistence of spine amelioration in older mice. Perseverative and repeated behaviors are thought to depend on corticostriatal circuits (Hill, 2004; Peca et al., 2011). Although we have not examined synaptic structure in the most anterior regions of the cortex, pro-inflammatory cytokines have been observed in the frontal cortex in MIA offspring (Garay et al., 2012). We have also confirmed *in vivo* that increased levels of surface MHCI proteins are expressed in the MIA offspring. Since immunological dysfunction in ASD and MIA offspring has been found both in the brain and in the peripheral immune system (Hsiao et al., 2012; Onore et al., 2014) our experiments cannot distinguish the site of action of ibudilast to affect the changes we report here. Moreover, effects of the drug on maternal behavior, gut microbiota (Hsiao et al., 2013) or epigenetic changes (Basil et al., 2014) have not been examined. Although a full pharmacokinetic analysis was beyond the scope of this study and therefore the peak levels of ibudilast reached in the offspring using lactation as a method of administration are unknown, we did determine using LC-MS that ibudilast was detected in both serum and brains of offspring mice 5 h following injection of lactating dams. Our data suggest therefore that reduction in inflammatory cytokines during the period of synaptogenesis in MIA offspring has long lasting effects indicating a therapeutic potential of ibudilast in treating MIA induced neurodevelopmental disorders.

Acknowledgments — We would like to thank Woo-Yang Kim for discussion and insightful comments on the manuscript. This work was supported by DOD/CDMRP Award W81XWH-13-1-0440, Nebraska Research Initiative and DHHS/NIH P20RR018788.

Appendix A. Supplementary data — Supplementary data associated with this article can be found following the References.

References

Ashwood, P., Krakowiak, P., Hertz-Picciotto, I., Hansen, R., Pessah, I., Van de Water, A., 2011. Elevated plasma cytokines in autism spectrum disorders provide evidence of immune dysfunction and are associated with impaired behavioral outcome. Brain Behav. Immun. 25, 40–45.

Atladottir, H.O., Thorsen, P., Ostergaard, L., Schendel, D.E., Lemcke, S., Abdallah, M., Parner, E.T., 2010. Maternal infection requiring hospitalization during pregnancy and autism spectrum disorders. J. Autism Dev. Disord. 40, 1423– 1430.

Basil, P., Li, Q., Dempster, E.L., Mill, J., Sham, P.C., Wong, C.C., McAlonan, G.M., 2014. Prenatal maternal immune activation causes epigenetic differences in adolescent mouse brain. Trans. Psychiatry 4, e434.

Bauman, M.D., Iosif, A.M., Smith, S.E., Bregere, C., Amaral, D.G., Patterson, P.H., 2014. Activation of the maternal immune system during pregnancy alters behavioral development of rhesus monkey offspring. Biol. Psychiatry 75, 332–341.

Borrell, J., Vela, J.M., Arevalo-Martin, A., Molina-Holgado, E., Guaza, C., 2002. Prenatal immune challenge disrupts sensorimotor gating in adult rats. Implications for the etiopathogenesis of schizophrenia. Neuropsychopharmacology 26, 204–215.

Brown, A.S., 2012. Epidemiologic studies of exposure to prenatal infection and risk of schizophrenia and autism. Dev. Neurobiol. 72, 1272–1276.

Chen, J.L., Nedivi, E., 2013. Highly specific structural plasticity of inhibitory circuits in the adult neocortex. Neuroscientist 19, 384–393.

Chen, J.L., Villa, K.L., Cha, J.W., So, P.T., Kubota, Y., Nedivi, E., 2012. Clustered dynamics of inhibitory synapses and dendritic spines in the adult neocortex. Neuron 74, 361–373.

Chez, M.G., Dowling, T., Patel, P.B., Khanna, P., Kominsky, M., 2007. Elevation of tumor necrosis factor-alpha in cerebrospinal fluid of autistic children. Pediatr. Neurol. 36, 361–365.

Comery, T.A., Harris, J.B., Willems, P.J., Oostra, B.A., Irwin, S.A., Weiler, I.J., Greenough, W.T., 1997. Abnormal dendritic spines in fragile X knockout mice. maturation and pruning deficits. Proc. Natl. Acad. Sci. U.S.A. 94, 5401–5404.

Costes, S.V., Daelemans, D., Cho, E.H., Dobbin, Z., Pavlakis, G., Lockett, S., 2004. Automatic and quantitative measurement of protein-protein colocalization in live cells. Biophys. J. 86, 3993–4003.

Cruz-Martin, A., Crespo, M., Portera-Cailliau, C., 2010. Delayed stabilization of dendritic spines in fragile X mice. J. Neurosci. 30, 7793–7803.

Dailey, M.E., Smith, S.J., 1996. The dynamics of dendritic structure in developing hippocampal slices. J. Neurosci. 16, 2983–2994.

Dani, V.S., Chang, Q., Maffei, A., Turrigiano, G.G., Jaenisch, R., Nelson, S.B., 2005. Reduced cortical activity due to a shift in the balance between excitation and inhibition in a mouse model of Rett syndrome. Proc. Natl. Acad. Sci. U.S.A. 102, 12560–12565.

De Gois, S., Schafer, M.K., Defamie, N., Chen, C., Ricci, A., Weihe, E., Varoqui, H., Erickson, J.D., 2005. Homeostatic scaling of vesicular glutamate and GABA transporter expression in rat neocortical circuits. J. Neurosci. 25, 7121–7133.

Dickerson, D.D., Overeem, K.A., Wolff, A.R., Williams, J.M., Abraham, W.C., Bilkey, D.K., 2014. Association of aberrant neural synchrony and altered GAD67 expression following exposure to maternal immune activation, a risk factor for schizophrenia. Trans. Psychiatry 4, e418.

Dunaevsky, A., Tashiro, A., Majewska, A., Mason, C., Yuste, R., 1999. Developmental regulation of spine motility in the mammalian central nervous system. Proc. Natl. Acad. Sci. U.S.A. 96, 13438–13443.

Ehninger, D., Sano, Y., de Vries, P.J., Dies, K., Franz, D., Geschwind, D.H., Kaur, M., Lee, Y.S., Li, W., Lowe, J.K., Nakagawa, J.A., Sahin, M., Smith, K., Whittemore, V., Silva, A.J., 2012. Gestational immune activation and Tsc2 haploinsufficiency cooperate to disrupt fetal survival and may perturb social behavior in adult mice. Mol. Psychiatry 17, 62–70.

Elmer, B.M., Estes, M.L., Barrow, S.L., McAllister, A.K., 2013. MHCI requires MEF2 transcription factors to negatively regulate synapse density during development and in disease. J. Neurosci. 33, 13791–13804.

Fatemi, S.H., Emamian, E.S., Sidwell, R.W., Kist, D.A., Stary, J.M., Earle, J.A., Thuras, P., 2002. Human influenza viral infection in utero alters glial fibrillary acidic protein immunoreactivity in the developing brains of neonatal mice. Mol. Psychiatry 7, 633–640.

Feng, G., Mellor, R.H., Bernstein, M., Keller-Peck, C., Nguyen, Q.T., Wallace, M., Nerbonne, J.M., Lichtman, J.W., Sanes, J.R., 2000. Imaging neuronal subsets in transgenic mice expressing multiple spectral variants of GFP. Neuron 28, 41–51.

Fiala, J.C., Spacek, J., Harris, K.M., 2002. Dendritic spine pathology: cause or consequence of neurological disorders? Brain Res. Brain Res. Rev. 39, 29–54.

Garay, P.A., Hsiao, E.Y., Patterson, P.H., Kimberley McAllister, A., 2012. Maternal immune activation causes age- and region-specific changes in brain cytokines in offspring throughout development. Brain Behav. Immun.

Garey, L.J., Ong, W.Y., Patel, T.S., Kanani, M., Davis, A., Mortimer, A.M., Barnes, T.R., Hirsch, S.R., 1998. Reduced dendritic spine density on cerebral cortical pyramidal neurons in schizophrenia. J. Neurol. Neurosurg. Psychiatry 65, 446– 453.

Girgis, R.R., Kumar, S.S., Brown, A.S., 2014. The cytokine model of schizophrenia: Emerging therapeutic strategies. Biol. Psychiatry 75, 292–299.

Glantz, L.A., Lewis, D.A., 2000. Decreased dendritic spine density on prefrontal cortical pyramidal neurons in schizophrenia. Arch. Gen. Psychiatry 57, 65–73.

Glynn, M.W., Elmer, B.M., Garay, P.A., Liu, X.B., Needleman, L.A., El-Sabeawy, F., McAllister, A.K., 2011. MHCI negatively regulates synapse density during the establishment of cortical connections. Nat. Neurosci. 14, 442–451.

Grant, S.G., 2012. Synaptopathies: diseases of the synaptome. Curr. Opin. Neurobiol. Grutzendler, J., Kasthuri, N., Gan, W.B., 2002. Long-term dendritic spine stability in the adult cortex. Nature 420, 812–816.

Hagberg, H., Gressens, P., Mallard, C., 2012. Inflammation during fetal and neonatal life: implications for neurologic and neuropsychiatric disease in children and adults. Ann. Neurol. 71, 444–457.

Hallmayer, J., Cleveland, S., Torres, A., Phillips, J., Cohen, B., Torigoe, T., Miller, J., Fedele, A., Collins, J., Smith, K., Lotspeich, L., Croen, L.A., Ozonoff, S., Lajonchere, C., Grether, J.K., Risch, N., 2011. Genetic heritability and shared environmental factors among twin pairs with autism. Arch. Gen. Psychiatry 68, 1095–1102.

Harrison, P.J., Eastwood, S.L., 2001. Neuropathological studies of synaptic connectivity in the hippocampal formation in schizophrenia. Hippocampus 11, 508–519.

Hill, E.L., 2004. Executive dysfunction in autism. Trends Cogn. Sci. 8, 26–32.

Holtmaat, A.J., Trachtenberg, J.T., Wilbrecht, L., Shepherd, G.M., Zhang, X., Knott, G.W., Svoboda, K., 2005. Transient and persistent dendritic spines in the neocortex in vivo. Neuron 45, 279–291.

Hsiao, E.Y., McBride, S.W., Chow, J., Mazmanian, S.K., Patterson, P.H., 2012. Modeling an autism risk factor in mice leads to permanent immune dysregulation. Proc. Natl. Acad. Sci. U.S.A. 109, 12776–12781.

Hsiao, E.Y., McBride, S.W., Hsien, S., Sharon, G., Hyde, E.R., McCue, T., Codelli, J.A., Chow, J., Reisman, S.E., Petrosino, J.F., Patterson, P.H., Mazmanian, S.K., 2013. Microbiota modulate behavioral and physiological abnormalities associated with neurodevelopmental disorders. Cell 155, 1451–1463.

Hur, E.E., Zaborszky, L., 2005. Vglut2 afferents to the medial prefrontal and primary somatosensory cortices: A combined retrograde tracing in situ hybridization study [corrected]. J. Comp. Neurol. 483, 351–373.

Hutsler, J.J., Zhang, H., 2010. Increased dendritic spine densities on cortical projection neurons in autism spectrum disorders. Brain Res. 1309, 83–94.

Ito, H.T., Smith, S.E., Hsiao, E., Patterson, P.H., 2010. Maternal immune activation alters nonspatial information processing in the hippocampus of the adult offspring. Brain Behav. Immun. 24, 930–941.

Jiang, M., Ash, R.T., Baker, S.A., Suter, B., Ferguson, A., Park, J., Rudy, J., Torsky, S.P., Chao, H.T., Zoghbi, H.Y., Smirnakis, S.M., 2013. Dendritic arborization and spine dynamics are abnormal in the mouse model of MECP2 duplication syndrome. J. Neurosci. 33, 19518–19533.

Kim, I.H., Racz, B., Wang, H., Burianek, L., Weinberg, R., Yasuda, R., Wetsel, W.C., Soderling, S.H., 2013. Disruption of Arp2/3 results in asymmetric structural plasticity of dendritic spines and progressive synaptic and behavioral abnormalities. J. Neurosci. 33, 6081–6092.

Knott, G.W., Holtmaat, A., Wilbrecht, L., Welker, E., Svoboda, K., 2006. Spine growth precedes synapse formation in the adult neocortex in vivo. Nat. Neurosci. 9, 1117–1124.

Knuesel, I., Chicha, L., Britschgi, M., Schobel, S.A., Bodmer, M., Hellings, J.A., Toovey, S., Prinssen, E.P., 2014. Maternal immune activation and abnormal brain development across CNS disorders. Nat. Rev. Neurol. 10, 643–660.

Krstic, D., Madhusudan, A., Doehner, J., Vogel, P., Notter, T., Imhof, C., Manalastas, A., Hilfiker, M., Pfister, S., Schwerdel, C., Riether, C., Meyer, U., Knuesel, I., 2012. Systemic immune challenges trigger and drive Alzheimer-like neuropathology in mice. J. Neuroinflammation 9, 151.

Kubota, Y., Hatada, S., Kondo, S., Karube, F., Kawaguchi, Y., 2007. Neocortical inhibitory terminals innervate dendritic spines targeted by thalamocortical afferents. J. Neurosci. 27, 1139–1150.

Landi, S., Putignano, E., Boggio, E.M., Giustetto, M., Pizzorusso, T., Ratto, G.M., 2011. The short-time structural plasticity of dendritic spines is altered in a model of Rett syndrome. Sci. Rep. 1, 45.

Ledeboer, A., Liu, T., Shumilla, J.A., Mahoney, J.H., Vijay, S., Gross, M.I., Vargas, J.A., Sultzbaugh, L., Claypool, M.D., Sanftner, L.M., Watkins, L.R., Johnson, K.W., 2006. The glial modulatory drug AV411 attenuates mechanical allodynia in rat models of neuropathic pain. Neuron Glia Biol. 2, 279–291.

Lee, F.H., Fadel, M.P., Preston-Maher, K., Cordes, S.P., Clapcote, S.J., Price, D.J., Roder, J.C., Wong, A.H., 2011. Disc1 point mutations in mice affect development of the cerebral cortex. J. Neurosci. 31, 3197–3206.

Malkova, N.V., Yu, C.Z., Hsiao, E.Y., Moore, M.J., Patterson, P.H., 2012. Maternal immune activation yields offspring displaying mouse versions of the three core symptoms of autism. Brain Behav. Immun. 26, 607–616.

Marin-Padilla, M., 1972. Structural abnormalities of the cerebral cortex in human chromosomal aberrations: A Golgi study. Brain Res. 44, 625–629.

McAlonan, G.M., Li, Q., Cheung, C., 2010. The timing and specificity of prenatal immune risk factors for autism modeled in the mouse and relevance to schizophrenia. Neurosignals 18, 129–139.

Meyer, U., Nyffeler, M., Engler, A., Urwyler, A., Schedlowski, M., Knuesel, I., Yee, B.K., Feldon, J., 2006. The time of prenatal immune challenge determines the specificity of inflammation-mediated brain and behavioral pathology. J. Neurosci. 26, 4752–4762.

Missault, S., Van den Eynde, K., Vanden Berghe, W., Fransen, E., Weeren, A., Timmermans, J.P., Kumar-Singh, S., Dedeurwaerdere, S., 2014. The risk for behavioural deficits is determined by the maternal immune response to prenatal immune challenge in a neurodevelopmental model. Brain Behav. Immun. 42, 138–146.

Mizuno, T., Kurotani, T., Komatsu, Y., Kawanokuchi, J., Kato, H., Mitsuma, N., Suzumura, A., 2004. Neuroprotective role of phosphodiesterase inhibitor ibudilast on neuronal cell death induced by activated microglia. Neuropharmacology 46, 404–411.

Morgan, J.T., Chana, G., Pardo, C.A., Achim, C., Semendeferi, K., Buckwalter, J., Courchesne, E., Everall, I.P., 2010. Microglial activation and increased microglial density observed in the dorsolateral prefrontal cortex in autism. Biol. Psychiatry 68, 368–376.

Olmos-Serrano, J.L., Paluszkiewicz, S.M., Martin, B.S., Kaufmann, W.E., Corbin, J.G., Huntsman, M.M., 2010. Defective GABAergic neurotransmission and pharmacological rescue of neuronal hyperexcitability in the amygdala in a mouse model of fragile X syndrome. J. Neurosci. 30, 9929–9938.

Onore, C.E., Schwartzer, J.J., Careaga, M., Berman, R.F., Ashwood, P., 2014. Maternal immune activation leads to activated inflammatory macrophages in offspring. Brain Behav. Immun. 38, 220–226.

Pacheco-Lopez, G., Giovanoli, S., Langhans, W., Meyer, U., 2013. Priming of metabolic dysfunctions by prenatal immune activation in mice: Relevance to schizophrenia. Schizophr. Bull. 39, 319–329.

Padmashri, R., Reiner, B.C., Suresh, A., Spartz, E., Dunaevsky, A., 2013. Al-

tered structural and functional synaptic plasticity with motor skill learning in a mouse model of fragile X syndrome. J. Neurosci. 33, 19715–19723.

Pan, F., Aldridge, G.M., Greenough, W.T., Gan, W.B., 2010. Dendritic spine instability and insensitivity to modulation by sensory experience in a mouse model of fragile X syndrome. Proc. Natl. Acad. Sci. U.S.A. 107, 17768–17773.

Patterson, P.H., 2009. Immune involvement in schizophrenia and autism: Etiology, pathology and animal models. Behav. Brain Res. 204, 313–321.

Patterson, P.H., 2011. Maternal infection and immune involvement in autism. Trends Mol. Med. 17, 389–394.

Peca, J., Feng, G., 2012. Cellular and synaptic network defects in autism. Curr. Opin. Neurobiol.

Peca, J., Feliciano, C., Ting, J.T., Wang, W., Wells, M.F., Venkatraman, T.N., Lascola, C.D., Fu, Z., Feng, G., 2011. Shank3 mutant mice display autistic-like behaviours and striatal dysfunction. Nature 472, 437–442.

Penzes, P., Cahill, M.E., Jones, K.A., VanLeeuwen, J.E., Woolfrey, K.M., 2011. Dendritic spine pathology in neuropsychiatric disorders. Nat. Neurosci. 14, 285–293.

Pologruto, T.A., Sabatini, B.L., Svoboda, K., 2003. ScanImage: Flexible software for operating laser scanning microscopes. Biomed. Eng. Online 2, 13.

Rolan, P., Hutchinson, M., Johnson, K., 2009. Ibudilast: A review of its pharmacology, efficacy and safety in respiratory and neurological disease. Expert Opin. Pharmacother. 10, 2897–2904.

Selemon, L.D., Goldman-Rakic, P.S., 1999. The reduced neuropil hypothesis: A circuit based model of schizophrenia. Biol. Psychiatry 45, 17–25.

Shi, L., Fatemi, S.H., Sidwell, R.W., Patterson, P.H., 2003. Maternal influenza infection causes marked behavioral and pharmacological changes in the offspring. J. Neurosci. 23, 297–302.

Snider, S.E., Hendrick, E.S., Beardsley, P.M., 2013. Glial cell modulators attenuate methamphetamine self-administration in the rat. Eur. J. Pharmacol. 701, 124– 130.

Suzumura, A., Ito, A., Yoshikawa, M., Sawada, M., 1999. Ibudilast suppresses TNFalpha production by glial cells functioning mainly as type III phosphodiesterase inhibitor in the CNS. Brain Res. 837, 203–212.

Thomas, A., Burant, A., Bui, N., Graham, D., Yuva-Paylor, L.A., Paylor, R., 2009. Marble burying reflects a repetitive and perseverative behavior more than novelty-induced anxiety. Psychopharmacology 204, 361–373.

Trachtenberg, J.T., Chen, B.E., Knott, G.W., Feng, G., Sanes, J.R., Welker, E., Svoboda, K., 2002. Long-term in vivo imaging of experience-dependent synaptic plasticity in adult cortex. Nature 420, 788–794.

Tropea, D., Giacometti, E., Wilson, N.R., Beard, C., McCurry, C., Fu, D.D., Flannery, R., Jaenisch, R., Sur, M., 2009. Partial reversal of Rett Syndrome-like symptoms in MeCP2 mutant mice. Proc. Natl. Acad. Sci. U.S.A. 106, 2029–2034.

Vargas, D.L., Nascimbene, C., Krishnan, C., Zimmerman, A.W., Pardo, C.A., 2005. Neuroglial activation and neuroinflammation in the brain of patients with autism. Ann. Neurol. 57, 67–81.

Voineagu, I., Wang, X., Johnston, P., Lowe, J.K., Tian, Y., Horvath, S., Mill, J., Cantor, R.M., Blencowe, B.J., Geschwind, D.H., 2011. Transcriptomic analysis of autistic brain reveals convergent molecular pathology. Nature 474, 380–384.

Volk, D.W., Pierri, J.N., Fritschy, J.M., Auh, S., Sampson, A.R., Lewis, D.A., 2002. Reciprocal alterations in pre- and postsynaptic inhibitory markers at chandelier cell inputs to pyramidal neurons in schizophrenia. Cereb. Cortex 12, 1063– 1070.

Wallace, M.L., Burette, A.C., Weinberg, R.J., Philpot, B.D., 2012. Maternal loss of Ube3a produces an excitatory/inhibitory imbalance through neuron type-specific synaptic defects. Neuron 74, 793–800.

Watanabe, Y., Someya, T., Nawa, H., 2010. Cytokine hypothesis of schizophrenia pathogenesis: Evidence from human studies and animal models. Psychiatry Clin. Neurosci. 64, 217–230.

Wei, H., Zou, H., Sheikh, A.M., Malik, M., Dobkin, C., Brown, W.T., Li, X., 2011. IL-6 is increased in the cerebellum of autistic brain and alters neural cell adhesion, migration and synaptic formation. J. Neuroinflammation 8, 52.

Willi, R., Harmeier, A., Giovanoli, S., Meyer, U., 2013. Altered GSK3beta signaling in an infection-based mouse model of developmental neuropsychiatric disease. Neuropharmacology 73, 56–65.

Xu, T., Yu, X., Perlik, A.J., Tobin, W.F., Zweig, J.A., Tennant, K., Jones, T., Zuo, Y., 2009. Rapid formation and selective stabilization of synapses for enduring motor memories. Nature 462, 915–919.

Zikopoulos, B., Barbas, H., 2013. Altered neural connectivity in excitatory and inhibitory cortical circuits in autism. Front. Hum. Neurosci. 7, 609.

Supplemental Material

Supplementary Method:

LC-MS/MS measurement of transmission of ibudilast through lactation. Lactating mothers were injected with 30mg/Kg ibudilast daily for 2 weeks starting one day after parturition. Five hours after the last injection, blood and brain were collected from the offspring. The blood was allowed to clot for 30 min after which it was centrifuged at 15,000 rpm for 15 min and serum was collected and frozen. Brains were homogenized in lysis buffer containing protease inhibitors, carried out with 3 cycles of sonication and centrifuged at 14,000 rpm for 20 minutes at 4°C. The protein concentration was determined using a BCA assay (Pierce, Thermo Scientific). Liquid chromatography/tandem mass spectrometry (LC-MS/MS) was used for ibudilast serum and brain sample analysis. A Waters ACQUITY UPLC system (Waters, Milford, MA) coupled to an Applied Biosystem 4000 Q TRAP®quadrupole linear ion trap hybrid mass spectrometer with an electrospray ionization (ESI) source (Applied Biosystems/MDS Sciex, Foster City, CA) was used. MS/MS analyses were performed in positive electrospray ionization mode; specific detection of ibudilast was performed by monitoring the transition 231.1→161.1 m/z. UPLC separation was carried out using an ACQUITY UPLC®BEH Shield RP 18 column with a isocratic mobile phase of 0.1% formic acid: acetonitrile (1:1, v/v) at a flow rate of 0.25 mL/min. For sample preparation, 1 mL of ice-cold acetonitrile was added to 50 µL serum or 100 µL brain homogenate samples. Samples were then vortexed and centrifuged at 16,000 g for 10 minutes. The supernatant was aspirated, evaporated under vacuum, and reconstituted in a 100 µL 50% acetonitrile. After centrifugation at 16,000 g for 10 minutes, 10 µL of each sample was used for LC-MS/MS analysis.

Supplemental Table 1: Dendritic parameters for the various experiments.

mean±sem

P17 Protrusion (Fig. 1)	**Con**	**MIA**
Total dendrite length (um)	1341	2500
Mean dendrite length (um)	37.4±3.5	35.8±2.4
Mean dendrite diameter (um)	1.1±0.04	1.07±0.02
Total number of spines	1338	1935

Colocalization (Fig. 3)	**Con**	**MIA**
Total dendrite length (um)	690	805
Mean dendrite length (um)	31.4±2.7	32.4±1.8
Mean dendrite diameter (um)	1.16±0.03	1.23±0.05
Total number of spines	661	574

P17 spines (Fig. 5)	**Con+Veh**	**MIA+Veh**	**Con+Ibud**	**MIA+Ibud**
Total dendrite length (um)	836.6	1078.	622.7	792.7
Mean dendrite length (um)	41.6±2.5	40.17±3.3	39.3±1.9	35.4±3.7
Mean dendrite diameter (um)	1.16±0.06	1.22±0.03	1.23±0.06	1.26±0.04
Total number of spines	751	825	559	727

Adult spines (Fig. 7)	**Con+Veh**	**MIA+Veh**	**Con+Ibud**	**MIA+Ibud**
Total dendrite length (um)	1446.4	1357.4	700.7	1153
Mean dendrite length (um)	43.26±1.4	44.6±1.9	38.2±3	45.74±3.1
Mean dendrite diameter (um)	1.08±0.02	1.07±0.014	1.2±0.07	1.17±0.05
Total number of spines	1226	794	517	869

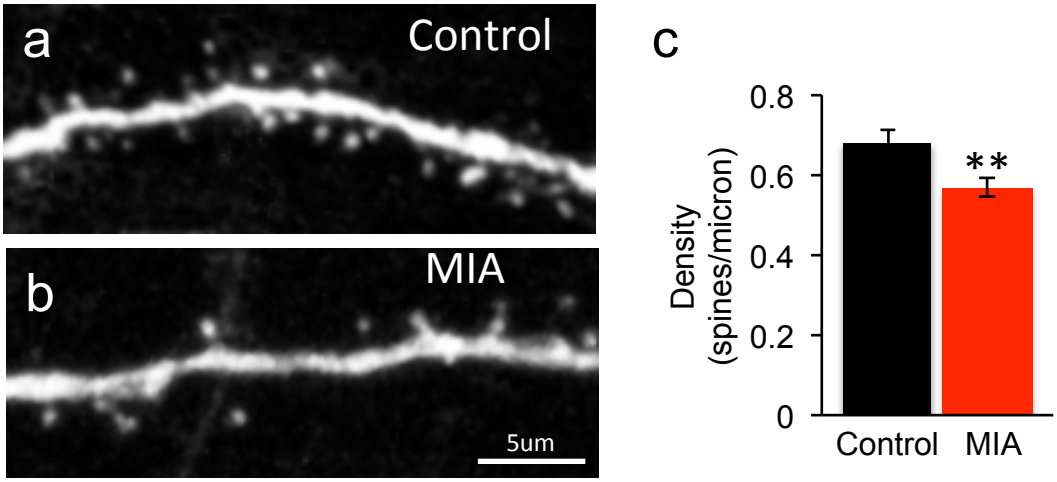

Supplemental Figure 1: MIA results in a reduction in total dendritic spine density on basal dendrites. Example images of basal dendrites from the somatosensory cortex in P30 **(a)** control and **(b)** MIA offspring. **c.** Spine densities in Control offspring 0.68±0.03 spines/μm, n= 48 images, 6 mice and MIA offspring 0.57±0.02, n= 58 images from 9 mice P=0.004, unpaired t-test.

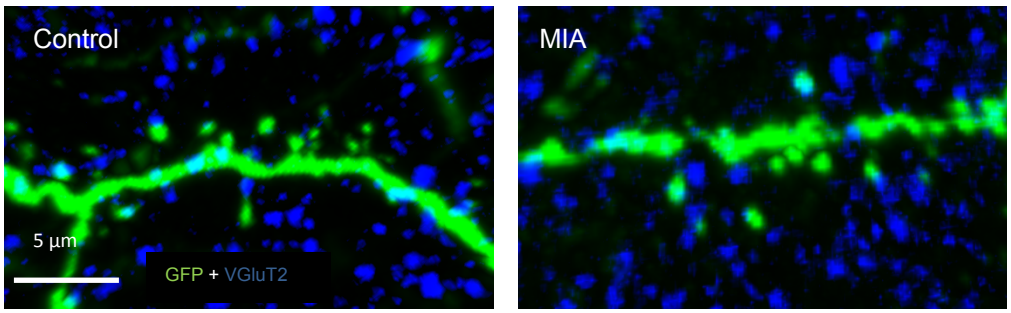

Supplemental Figure 2: VGluT2 staining in the cortex. Somatosensory sections from YFP-H P17 control and MIA offspring immunostained for VGluT2 and GAD-65.

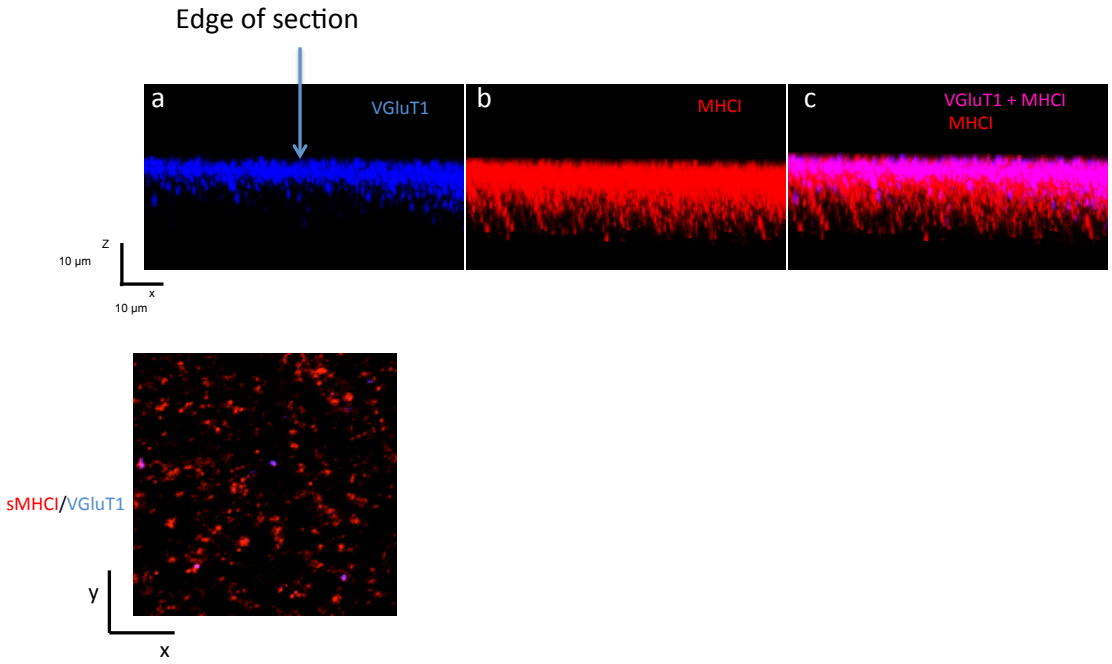

Supplemental Figure 3: In vivo analysis of surface expression of MHCI.

Side view (XZ) of VGluT1 (a) and MHCI (b) staining in unpermeabilized sections imaged on a confocal microscope. The top of the section is marked with an arrow. The portion of section in which VGluT1 and MHCI colocolized staining is detected (purple in c) is not considered for surface analysis. The MHCI staining found in focal planes immediately below the colocolized signal (as in the white box) is considered surface MHCI staining and is used for analysis.

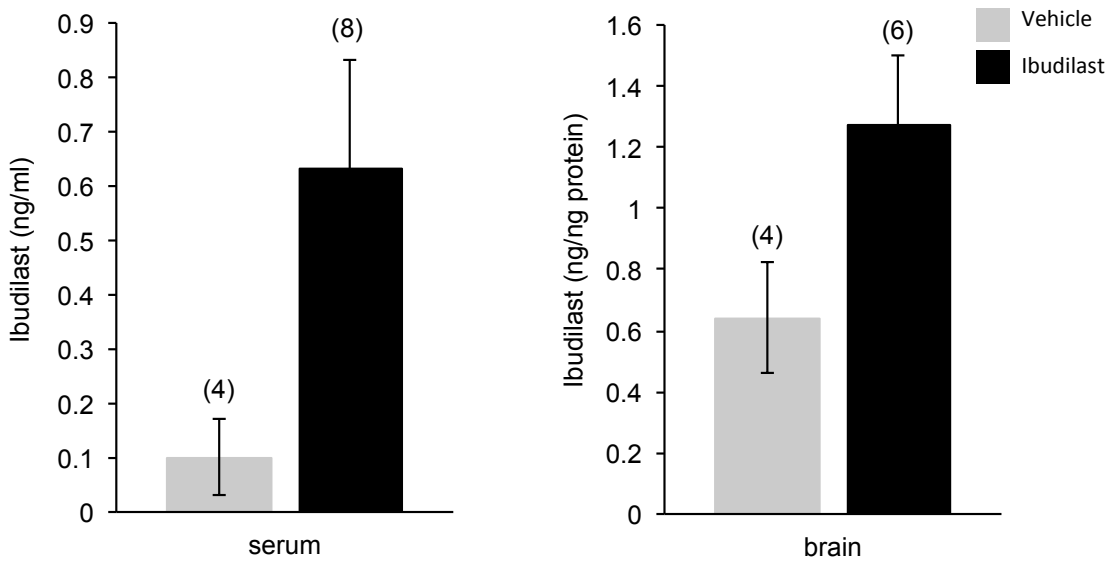

Supplemental Figure 4: Ibudilast can be detected in serum (ng/mL) and brain (ng/ng protein) of offspring following transmission of ibudilast through lactation. Mean ± SEM, number of pups used are indicated.

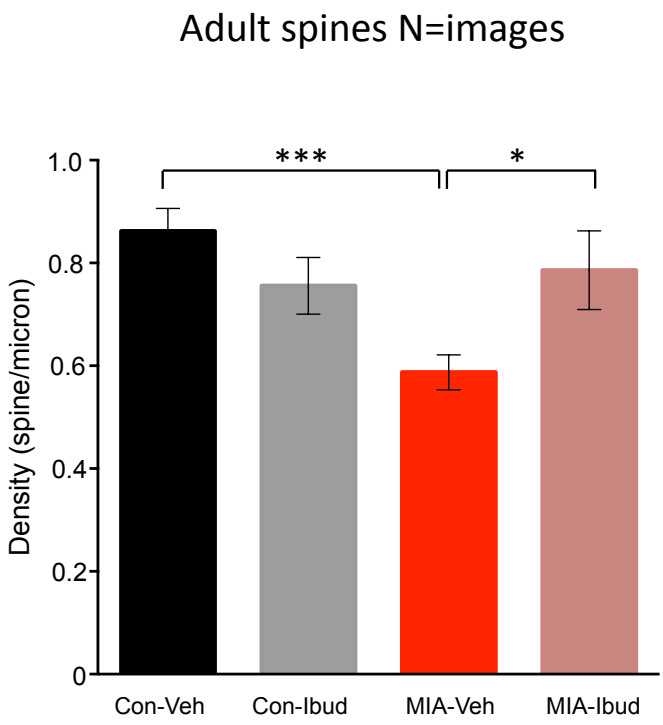

Supplemental Figure 5: Postnatal treatment with an anti-inflammatory drug prevents dendritic spine deficits. Same data as in figure 7b was analyzed with N=images. Two-way ANOVA was first used to test for the presence of interaction between drug treatment and experimental groups. This revealed an interaction consistent with the observation that ibudilast increased dendritic spine density in the MIA offspring but had no effect on the controls $F(1, 103)=7.953$, $P=0.006$. *Post hoc* two-way ANOVA with Bonferroni's correction indicates that a reduction in spine density in MIA+Vehicle offspring persists into adulthood (control + vehicle: 0.86±0.04 spines/micron, n=34 images; MIA + vehicle: 0.58±0.03 spines/micron, n=30 images, $P=0.0006$,) but is prevented by postnatal treatment with the anti-inflammatory drug Ibudilast (MIA + Ibudilast: 0.78±0.07 ± spines/micron, n=25 images, MIA + vehicle: 0.58± 0.03 spines/micron, n=30 images, $P=0.04$). No changes in spines density in control+ibudilast offspring (control + vehicle: 0.86±0.04 spines/micron, n=34 images; control + ibudilast: 0.75±0.05 spines/micron, n=18 images, $P=0.45$).

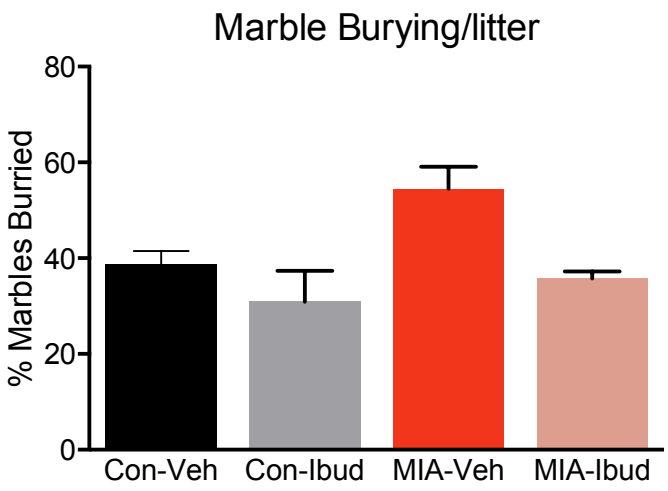

Supplemental Figure 6: Marble burying is increased in MIA offspring and is reduced by Ibudilast. Because for the behavioral data 2-5 mice per litter were used the data presented in Figure 7c is compiled here while considering litters as independent variable. There was a main effect of prenatal treatment, $F(1,12)=5.84$, $P=0.03$, as well as a main effect of drug treatment, $F(1,12)=9.67$, $P=0.009$ on marble burying but no significant interaction $F(1,12)=1.63$, $P=0.22$. Marble burying increased in MIA offspring (con+veh: 38.73±2.76%, n= 4 litters; MIA+veh: 54.48±4.6%, n=4 litters). This increase is reduced in MIA offspring treated with ibudilast during the first 2 postnatal weeks (MIA+Ibud: 35.78±1.46%, n=4 litters). There was a mild effect of Ibudilast on control offspring (con+Ibud: 30.96±6.4%, n=4 litters).